Journal of Computational Neuroscience 1, 69–87 (1994).

Mechanisms for Oscillation and Frequency Control in Reciprocally Inhibitory Model Neural Networks

FRANCES K. SKINNER* SKINNER@BINAH.CC.BRANDEIS.EDU
Department of Biology and Center for Complex Systems, Brandeis University, Waltham, MA 02254-9110

NANCY KOPELL
Department of Mathematics, Boston University, Boston, MA 02215

EVE MARDER
Department of Biology and Center for Complex Systems, Brandeis University, Waltham, MA 02254-9110

Received September 27, 1993; Revised February 28, 1994; Accepted (in revised form) March 22, 1994

Action Editor: T. Williams

Abstract. We describe four different mechanisms that lead to oscillations in a network of two reciprocally inhibitory cells. In two cases (intrinsic release and intrinsic escape) the frequency of the network oscillation is insensitive to the threshold voltage of the synaptic potentials. In the other two cases (synaptic release and synaptic escape) the network frequency is strongly determined by the threshold voltage of the synaptic connections. The distinction between the different mechanisms blurs as the function describing synaptic activation becomes less steep and as the model neurons are removed from the relaxation regime. These mechanisms provide insight into the parameters that control network frequency in motor systems that depend on reciprocal inhibition.

Introduction

Neurons have widely different intrinsic membrane properties that allow them to exhibit many different behaviours. They may be silent unless stimulated, display plateau properties or show bursting pacemaking properties (Harris-Warrick and Marder, 1991; Marder, 1993). It is known that neurons with oscillatory properties play important roles in the nervous system (Harris-Warrick and Marder, 1991; Jacklet, 1989; Llinás, 1988). However, it is often difficult to determine how the oscillatory properties of neurons influence the output of the networks in which they are embedded.

Rhythmic movements are often produced by networks with oscillatory or rhythmic outputs. These networks or central pattern generators are known to underlie behaviours such as respiration, heartbeat, swimming, feeding and other motor patterns (Delcomyn, 1980; Cohen et al., 1988; Jacklet, 1989). Rhythmic output could be produced by individual pacemaker cells, network interactions or a combination of the two (Selverston and Moulins, 1985; Getting, 1989a). For example, it has long been appreciated that rhythmic output could be generated by neurons that are connected by reciprocally inhibitory synapses, "half- center oscillators" (Brown, 1911), even when the individual neurons themselves were not oscillatory. However, it is not clearly understood how the rhythmic output is controlled. Oscillations produced by networks of reciprocally inhibitory neurons are integral to several pattern generating circuits (e.g., Arshavsky et al., 1993; Calabrese and DeSchutter, 1992; Satterlie, 1985), and therefore it is important to understand what properties determine the network frequency and therefore

*Please address all correspondence to Frances K. Skinner at the above address. 617-736-3134 (Phone), 617-736-3142 (Fax).

the period of the controlled movement.

In this paper, we show that there are at least four different mechanisms that lead to oscillation in a network of two reciprocally inhibitory cells. Two of these are determined by the intrinsic properties of the neurons, and the other two are determined by the properties of the synapses. We show that for the mechanisms involving the synapses, the frequency of the network depends critically on the synaptic threshold voltage; for the intrinsic mechanisms, the synaptic threshold voltage does not have a significant impact on the network frequency. The mechanisms we identify extend and refine ideas in Wang and Rinzel (1992).

The analysis of the mechanisms is done using restrictions on the network elements and the coupling between them. The network elements are assumed to be of a relaxation type, i.e., with some processes that occur on a much faster time scale than others. The synaptic coupling is assumed to have a sharp threshold and a fast time constant. If some of these assumptions are relaxed, the qualitative behaviour remains similar, but the distinction between the four mechanisms becomes less sharp.

In a previous paper (Skinner et al., 1993) we described how the behaviour of two cell reciprocally inhibitory networks can change as the parameter representing injected current is increased. Simulations in that paper showed that if sufficient current is injected into each cell, the rhythm stops; a further injection of current then restarts the rhythm. The analysis in this paper clarifies those simulations by showing how the current injection changes the ability of the network to oscillate and the mechanism underlying the oscillatory behaviour.

Methods

Basic Geometry

Our analysis applies to classes of neural-like equations with similar geometry, independent of the ionic currents that underlie that geometry. For simplicity, we shall describe the geometry in two- dimensional equations, though the description can be extended to higher-dimensional equations.

Each of the two cells is assumed to be described by equations of the form:

$$\begin{aligned} \epsilon \dot{V} &= f(V,N) \\ \dot{N} &= g(V,N) \end{aligned} \tag{1}$$

where V denotes the voltage and N is the recovery or slow variable. Here the nullcline $f(V,N) = 0$ is assumed to have a shape that is qualitatively cubic, as in Figure 1. The nullcline $g(V,N) = 0$ is assumed to be sigmoidal, also as in Figure 1. The g nullcline is the same for all three parts of Figure 1. A well-known example of such equations are the Morris-Lecar equations (Morris and Lecar, 1981), which are used for the simulations done in this paper. These equations are sometimes used to model the envelope of the voltage traces of a bursting neuron.

With nullclines of these shapes, equations (1) can have a stable critical point as in Figures 1a and 1b, or a stable oscillation as in Figure 1c. In Figure 1a, the stable critical point is on the lowest branch of the cubic; this corresponds to equilibrium at rest potential in a bursting model. In Figure 1b, the critical point is on the highest branch, which corresponds to tonic firing when the equations are interpreted as envelope equations. Some trajectories are drawn in each case. Note that ϵ small implies that the trajectories stay close to the nullcline $f(V,N) = 0$ until they reach a local maximum or minimum, then jump quickly to another branch; in the limit $\epsilon \to 0$, the jump is instantaneous.

Coupling occurs via the voltages of the two oscillators. A term $h(V,\hat{V})$ is added to the first equation of (1), where $\hat{V}$ is the voltage of the other oscillator. We assume that $h(V,\hat{V})$ has the form $m(\hat{V})(V - V_{syn})$, a standard model of a fast chemical synapse. Here V_{syn} is the synaptic reversal potential, and is set so that the synaptic current is hyperpolarizing. For most of the paper, the function $m(\hat{V})$ is a step function: it is zero below some threshold V_{thresh} and is a positive constant above the threshold V_{thresh}. Thus $h(V,\hat{V}) = 0$ for $\hat{V} < V_{thresh}$ and $h(V,\hat{V}) = const.(V - V_{syn})$ for $V \geq V_{thresh}$. We

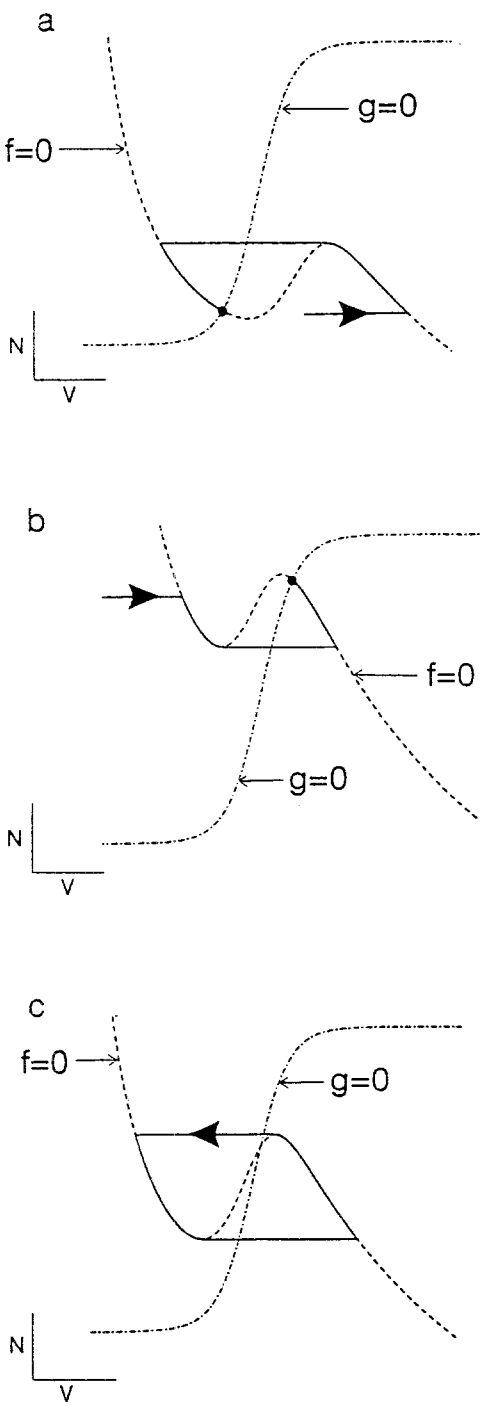

Fig. 1. The cubic-like nullcline $f = 0$ represents the steady-state behaviour of the V variable. The sigmoidal-like nullcline $g = 0$ represents the steady-state behaviour of the N variable, which is the slow variable. (a) The nullclines intersect on the lowest branch of the $f = 0$ nullcline. This results in a stable behaviour at a lower V value. (b) The nullclines intersect on the highest branch of the $f = 0$ nullcline. This results in a stable behaviour at a higher V value. (c) The nullclines intersect on the middle branch of the $f = 0$ nullclines. This results in an unstable critical point which gives stable oscillatory behaviour.

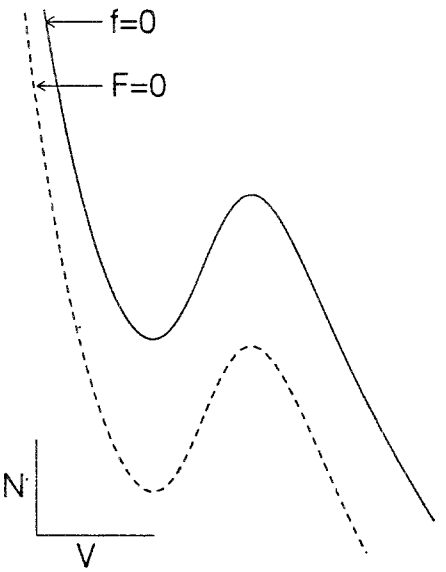

Fig. 2. Nullclines of free and inhibited systems. The cubic-like nullclines represent the points for which $\dot{V} = 0$. The solid line ($f = 0$) corresponds to the system without any inhibition and the dashed line ($F = 0$) corresponds to the system under constant inhibition.

let $F(V,N) = f(V,N) + const.(V - V_{syn})$. We refer to (1) with $f(V,N)$ replaced by $F(V,N)$ as the inhibited system, and $F(V,N) = 0$ as the voltage nullcline for the inhibited system. Note that the choice of V_{syn} implies that the $F(V,N) = 0$ nullcline lies below the $f(V,N) = 0$ nullcline, as shown in Figure 2.

Results

Mechanisms for Network Oscillations

The mechanisms will be illustrated with simulations using Morris-Lecar equations for each cell. The equations and the relevant parameters are shown in Appendix A.

Intrinsic Mechanisms

The first two mechanisms we describe depend on the intrinsic properties of the cells. Provided that the synaptic threshold, V_{thresh}, stays within some bounds that we will make explicit, we shall see that this threshold plays no role in determining either the waveform or the frequency of the network oscillations.

Release. This intrinsic release mechanism is illustrated in the phase plane portrait of Figure 3a. The sigmoidal shaped curve is the nullcline of the recovery variable. In particular, for the Morris-Lecar equations used here, the recovery variable represents the activation of the outward K^+ current and the nullcline is given by $g = 0$. The upper and lower cubic-like curves represent the voltage nullclines or $f = 0$ for the uninhibited system and $F = 0$ for the inhibited system. These curves are described in the previous section and are shown in Figures 1 and 2. The dashed line shows the synaptic threshold voltage. The trajectory for this intrinsic release mechanism is described as follows (see Figure 3a): During the network oscillation, the free cell reaches the end of its plateau marked as k^+, and jumps down to $j(k^+)$, releasing the inhibited cell. At that moment, the inhibited cell jumps to its excited plateau from p to $j(p)$. The corresponding voltage versus time plot is shown in Figure 3b for the two cells. Again, the dashed line in Figure 3b represents the synaptic threshold voltage.

This rhythm can happen even if neither the uninhibited system nor the inhibited one (i.e., the cell under sustained inhibition) is capable of autonomous oscillations. The main constraint for this mechanism is that the uninhibited cell not be tonically active. It may either oscillate or have a stable critical point; i.e., the $g = 0$ nullcline may not intersect the $f = 0$ nullcline on the right-hand branch. Figure 3a illustrates a case of intrinsic release in which the uninhibited cell is capable of autonomous oscillation. As shown in Figure 3a, the trajectory of the uninhibited cell reaches the maximum of the $f = 0$ nullcline, jumps downward, and thereby releases the inhibited cell to jump upward.

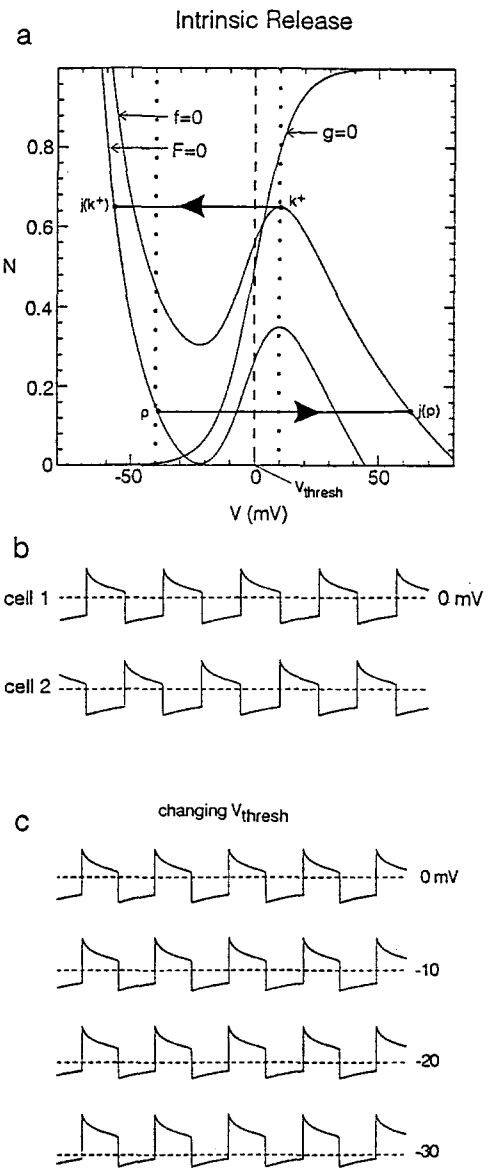

Fig. 3. Intrinsic Release Mechanism. (a) Phase-plane portrait, N versus V. There are two V-nullclines representing the free and inhibited systems and one N-nullcline which is the same for both free and inhibited cells. The synaptic threshold is 0 mV. The resulting trajectory passes through the local maximum of the uninhibited nullcline. (b) Voltage versus time for the two cells using a synaptic threshold voltage of 0 mV. (c) Voltage versus time for one cell using synaptic threshold voltages of −30, −20, −10 and 0 mV. The dashed line represents the synaptic threshold voltage. Model parameters are: $g_{\text{syn}} = 6\ \mu\text{S/cm}^2$, $I_{ext} = 0.4\ \mu\text{A/cm}^2$, $\phi_N = 0.000002\ \text{msec}^{-1}$, $V_{\text{slope}} = 0.001$ mV, and the other parameter values are shown in Appendix A.

We are mainly interested in rhythms in which the upjump of one cell coincides with the downjump of the other cell, i.e., the duty cycle is 1/2. In order that there be a trajectory with duty cycle 1/2 corresponding to intrinisic release, there is another condition: there must be a point p as in Figure 3a such that the time from $j(k^+)$ to p equals the time from $j(p)$ to k^+. This constraint determines the point p of the trajectory. See Appendix B for a discussion of the stability of the solution, as well as remarks on when there is such a value of p. If there is no such p, the behaviour can be more complicated. This is illustrated at the end of the Motivating Example section, and discussed further in Appendix B.

The only constraint on the synaptic threshold is that it lie between the rapid upstroke and rapid downstroke of the coupled system. The rapid upstroke and downstroke are represented by the dotted lines in Figure 3a. Within this range, changing the synaptic threshold has *no effect* on the periodic trajectory of the limiting $\epsilon \to 0$ system, and hence no effect on the period. This is clearly shown in Figure 3c where voltage versus time plots are shown for one of the cells at four different synaptic thresholds.

Escape. The phase plane portrait in Figure 4a illustrates the intrinsic escape mechanism. Similar to Figure 3a, in Figure 4a, the sigmoidal and cubic-like curves are the nullclines of the system and the dashed line represents the synaptic threshold voltage. The trajectory shown in Figure 4a is as follows: During the network oscillation, the inhibited cell reaches k^-, the end of its slow depolarization, and jumps up to $j(k^-)$ inhibiting the other cell. At that moment, the free cell jumps to its inhibited state from p to $j(p)$. The voltage versus time plot which corresponds to this trajectory is shown in Figure 4b for the two cells. The dashed line represents the synaptic threshold voltage.

The essential requirement for this mechanism is that the inhibited system be capable of oscillation or tonic activity; i.e., the $g = 0$ nullcline may not intersect the $F = 0$ nullcline on its left-hand branch. As before, in the $\epsilon \to 0$ limit, the periodic solution is completely independent of the synaptic threshold, provided that the latter

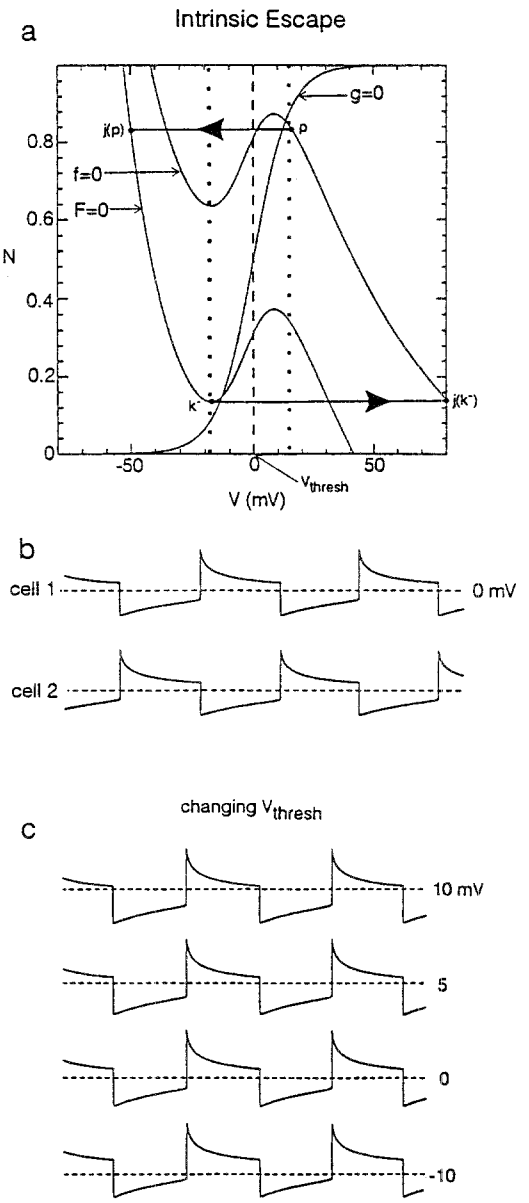

Fig. 4. Intrinsic Escape Mechanism. (a) Phase-plane portrait, N versus V. There are two V- nullclines representing the free and inhibited systems and one N- nullcline which is the same for both free and inhibited cells. The synaptic threshold is 0 mV. The resulting trajectory passes through the local minimum of the inhibited nullcline. (b) Voltage versus time for the two cells using a synaptic threshold voltage of 0 mV. (c) Voltage versus time for one cell using synaptic threshold voltages of -10, 0, 5, 10 mV. The dashed line represents the synaptic threshold voltage. Model parameters are: $g_{syn} = 10$ μS/cm^2, $I_{ext} = 0.8$ μA/cm^2, $\phi_N = 0.000002$ msec^{-1}, $V_{slope} = 0.001$ mV, and the other parameter values are shown in Appendix A.

is within the voltages of the rapid upstroke and rapid downstroke which again corresponds to the dotted lines in Figure 4a. For four different synaptic threshold voltages, the frequency and waveform do not change. This is shown in Figure 4c for one of the cells. As in the intrinsic release mechanism, there is a further restriction in order that there be a trajectory with duty cycle 1/2: there must be a point p on the right-hand branch of the $f = 0$ nullcline for which the time from $j(k^-)$ to p equals the time from $j(p)$ to k^-.

It has been pointed out (R. Calabrese, personal communication) that the case of intrinsic escape is especially interesting when neither the inhibited nor the uninhibited cell is an oscillator. In this mechanism, the inhibited cell recovers to a reduced level of tonic activity in the presence of continuous inhibition; in the reciprocal network, it can terminate the inhibition to return to full activity during a part of the network oscillation. This may correspond to an oscillator based on an h-current (Calabrese and DeSchutter, 1992).

Synaptic Mechanisms

The synaptic mechanisms come into operation when the synaptic threshold lies outside the interval between the upjump voltage and the downjump voltage for the coupled system, as represented by the dotted lines in Figures 3a and 4a above. The synaptic threshold may then lie on the interval of voltages corresponding to either the upper branch of the uninhibited nullcline or the lower branch of the inhibited nullcline. These two cases correspond to synaptic release or synaptic escape respectively.

Release. The synaptic release mechanism is shown in the phase plane portrait of Figure 5a. As before, the sigmoidal and cubic-like curves are the nullclines and the dashed line is the synaptic threshold voltage. For this case the upper branch of the free nullcline has voltages on both sides of the synaptic threshold. The jumps occur when the uninhibited cell's voltage declines to the synaptic threshold. The trajectory in Figure 5a can be described as fol-

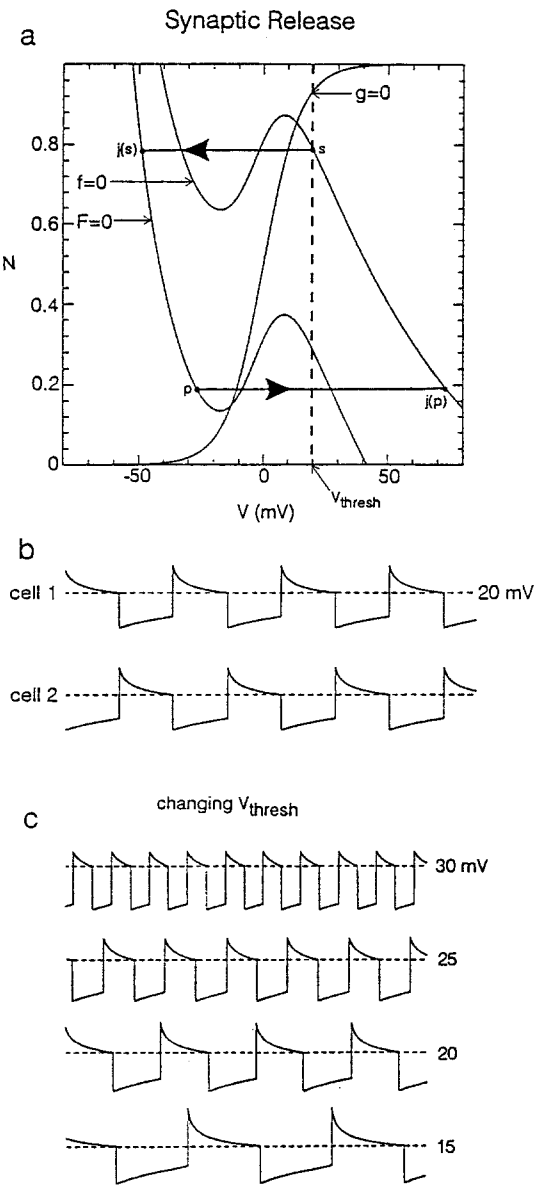

Fig. 5. Synaptic Release Mechanism. (a) Phase-plane portrait, N versus V. There are two V-nullclines representing the free and inhibited systems and one N-nullcline which is the same for both free and inhibited cells. The synaptic threshold is 20 mV. The resulting trajectory does not pass through either the local maximum or minimum of the voltage nullclines. (b) Voltage versus time for the two cells using a synaptic threshold voltage of 20 mV. (c) Voltage versus time for one cell using synaptic threshold voltages of 15, 20, 25, 30 mV. The dashed line represents the synaptic threshold voltage. Model parameters are given in Figure 4.

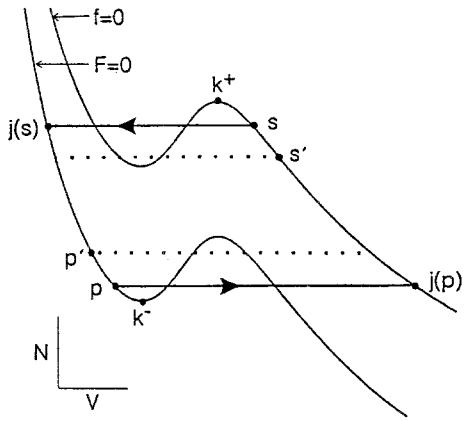

Fig. 6. Synaptic Release Mechanism. The two V-nullclines represent the free and inhibited systems. The trajectory goes through the points marked s, $j(s)$, p and $j(p)$.

lows: When the free cell of the coupled system reaches the synaptic threshold voltage, the free cell ceases to inhibit the other cell. The latter is now governed by the voltage nullcline of the free system, causing it to jump to the excited branch from p to $j(p)$, and thus to inhibit the first cell; the first cell is then constrained to jump downward at the point from s to $j(s)$. The point p in Figure 5a is determined by the requirement that the time from $j(p)$ to the synaptic threshold s equals the time from $j(s)$ to p. The voltage versus time oscillations which correspond to the trajectory in Figure 5a are shown in Figure 5b for the two cells.

The existence of the synaptic threshold on the upper branch of the free system, plus the inhibitory coupling, indirectly prevents the free oscillator from moving past that threshold. Figure 5a shows that the periodic solution does not pass through the local maxima or minima of the voltage nullclines (unlike the periodic solution for the intrinsic mechanisms). For this mechanism, the frequency and waveform are critically dependent on the synaptic threshold. This dependence is shown in Figure 5c where voltage versus time plots are shown for one of the cells at four different synaptic thresholds. There is a drastic *decrease* in network frequency as the synaptic threshold decreases.

The reason for the dependence of the period and waveform on s can be seen in Figure 6. As the voltage corresponding to s increases (to s' in Figure 6), the voltage corresponding to the point p decreases (to the point p'). This decreases the amplitude and period, as can be seen in Figure 5c.

Escape. In Figure 7a the phase plane portrait for the synaptic escape mechanism is illustrated. The curves representing the nullclines are the same as in the previous figures and again the synaptic threshold voltage is given by the dashed line. In this mechanism the lower branch of the inhibited nullcline contains voltages on both sides of the synaptic threshold.

The trajectory in Figure 7a is described by the following: When the inhibited cell passes the synaptic threshold, the voltage is large enough to inhibit the other cell. This causes the latter to be governed by the inhibited nullcline, and hence to jump down to the unexcited branch from p to $j(p)$. When it does this, the first cell can escape from inhibition, and it jumps upward from s to $j(s)$. The point p in Figure 7a is determined as in the release mechanism by the requirement that the time from $j(p)$ to s equals the time from $j(s)$ to p. The corresponding voltage versus time plot for the two cells is shown in Figure 7b.

The coupling indirectly allows the inhibited cell to escape and jump upward when it reaches the synaptic threshold. Again the solution does not pass through local maxima or minima of the voltage nullcline. Similar to the synaptic release case, the output generated via the synaptic escape mechanism is sensitive to the synaptic threshold. This sensitivity is shown in Figure 7c for one cell at four different synaptic thresholds. This time the network frequency drastically *increases* as the synaptic threshold decreases. The reason for the sensitivity is similar to that for synaptic release.

For the synaptic mechanisms, neither cell in the free nor the inhibited systems needs to be capable of exhibiting autonomous oscillations. Similar to Wang and Rinzel (1992), bistability in our mechanisms can occur in several ways. For example, if the steady state is on the upper branch of the $f = 0$ nullcline, as shown for the synaptic release example in Figure 5a, the network can either exhibit oscillatory behaviour as shown in Figure 5b or both cells can be stable

at the steady-state voltage of the free system. If the steady state is on the lower branch of the $F = 0$ nullcline in the synaptic escape mechanism, bistability will exist between the oscillatory state and this steady state. However, this is not the case for the synaptic escape example shown in Figure 7a.

In considering all four mechanisms, the escape cases can be thought of as occurring due to the initiative of the inhibited cell. The inhibited cell either escapes due to its intrinsic properties or because it starts inhibiting the other cell. The release cases can be thought of as occurring due to the initiative of the free cell. The free cell either reaches the end of its plateau by virtue of its intrinsic properties or it stops inhibiting the other cell, allowing the latter to be released. However, as shown above, whether the mechanism is escape or release does not determine the sensitivity of the network oscillation to the synaptic threshold. The four mechanisms are summarized in Table 1. The conditions for each mechanism, how the transition between on and off occurs and the effect of changing the synaptic threshold on network period are briefly described in this table.

In Figure 8 we show how frequency changes with synaptic threshold for the four mechanisms. The normalized period versus synaptic threshold voltage is plotted. The period is normalized such that at a synaptic threshold of 0 mV, the period is 1. The range of synaptic threshold values for which there is no period change corresponds to the region when the intrinsic mechanisms are in operation. However, where the synaptic mechanisms come into play, there is a significant change in period with synaptic threshold: The frequency increases with increasing synaptic threshold for the release case and the frequency decreases with increasing synaptic threshold for the escape case. Figure 8 gives frequency versus synaptic threshold for two different sets of parameters. For one set (the solid line), synaptic escape, intrinsic escape and synaptic release mechanisms are exhibited. This solid line corresponds to the nullclines shown in Figure 4a, 5a or 7a. For the other (the dashed line), synaptic escape, intrinsic release and synaptic release mechanisms are exhibited. This dashed line cor-

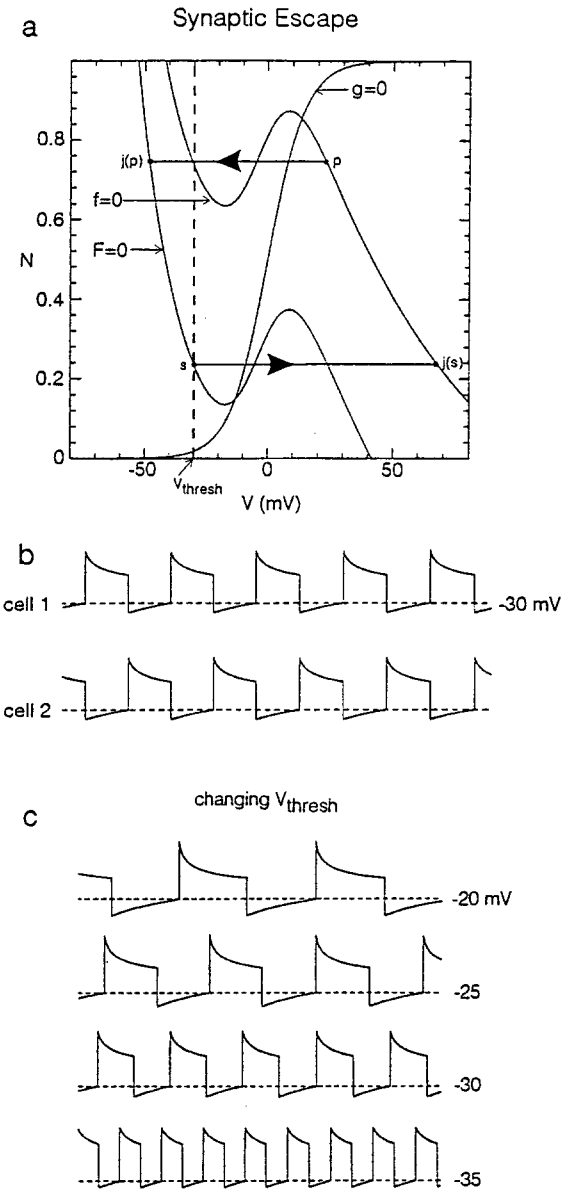

Fig. 7. Synaptic Escape Mechanism. (a) Phase-plane portrait, N versus V. There are two V- nullclines representing the free and inhibited systems and one N- nullcline which is the same for both free and inhibited cells. The synaptic threshold is −30 mV. The resulting trajectory does not pass through either the local maximum or minimum of the voltage nullclines. (b) Voltage versus time for the two cells using a synaptic threshold voltage of −30 mV. (c) Voltage versus time for one cell using synaptic threshold voltages of −35, −30, −25, −20 mV. The dashed line represents the synaptic threshold voltage. Model parameters are given in Figure 4.

Table 1. A Summary of the 4 mechanisms.

Mechanism	Conditions (on cells)	Conditions (on synaptic threshold)	How transition occurs	Effect of synaptic threshold on period
Intrinsic Release	Free cell must be endogenous burster or silent, not tonic.	Synaptic threshold must be more hyperpolarized than the voltage at which free cell's burst terminates or more depolarized than free cell's silent state.	Free cell reaches end of burst, terminates inhibition and allows inhibited cell to fire.	Period unchanged by change in synaptic threshold.
Intrinsic Escape	Inhibited cell must be endogenous burster or tonic, not silent.	Synaptic threshold must be more depolarized than voltage at which inhibited cell starts to burst or more hyperpolarized than inhibited cell's tonic state.	Inhibited cell generates burst and shuts off free cell.	Period unchanged by change in synaptic threshold.
Synaptic Release	Free cell must be tonic or endogenous burster, not silent.	Synaptic threshold must be more depolarized than tonic state of free cell and/or the voltage at which free cell's burst terminates.	Free cell drops below synaptic threshold and allows inhibited cell to depolarize.	Period increases when synaptic threshold decreases.
Synaptic Escape	Inhibited cell must be silent or endogenous burster, not tonic.	Synaptic threshold must be more hyperpolarized than inhibited cell's silent state and/or the voltage at which the inhibited cell starts to burst.	Inhibited cell crosses synaptic threshold and starts to inhibit free cell.	Period decreases when synaptic threshold decreases.

responds to the nullclines shown in Figure 3a.

Effects of Relaxing Assumptions

In the previous section, certain assumptions were made which allowed the distinction between the four mechanisms to be sharp. If we now relax some of the assumptions, then we find that the concepts developed above are still useful. The assumptions that we relax are (i) $\epsilon \ll 1$ which corresponds to the network elements being of relaxation type, and (ii) sharp synaptic thresholds or steep synaptic activations. We do not relax the assumption of a fast time constant for the synaptic coupling.

In Figure 9 we plot normalized period versus synaptic threshold for two cases. These cases correspond to the nullclines shown in Figures 4a, 5a or 7a. The solid line corresponds to parameters for which the oscillations are of relaxation type, i.e., some processes have a much faster time constant than others. The dashed line corresponds to parameters for which the oscillations are not of relaxation type. The only difference in parameter values between these two situations is in the time constant of one of the processes. Again, the period is normalized such that at a synaptic threshold of 0 mV, the period is 1.

As shown in Figure 9, if the oscillations are not of a relaxation type, then the frequency does change with synaptic threshold during the intrinsic mechanisms. However, the frequency variation is small when compared with the frequency variation during the synaptic mechanisms. Also, the switch between intrinsic and synaptic mechanisms does not occur at the same positions since now the voltage trajectories do not closely follow the nullclines.

The assumption made in the previous section, that there is a sharp synaptic threshold, means that the slope of the synaptic activation is very steep. For a synaptic threshold of 0 mV, the synaptic activation versus voltage is plotted in Figure 10b for four different slope values. The solid line represents the steepest slope or the sharpest threshold ($V_{\text{slope}} = 0.001$ mV). In this

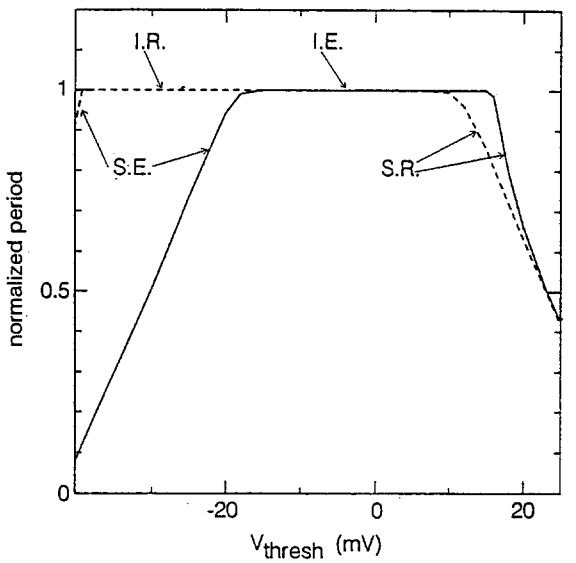

Fig. 8. Normalized period versus synaptic threshold voltage (V_{thresh}) for relaxation like oscillations and steep synaptic activation slopes. The period is normalized to 1 at 0 mV synaptic threshold voltage. Model parameters for the solid line are given in Figure 4. Model parameters for the dashed line are given in Figure 3. I.R. = Intrinsic Release, I.E. = Intrinsic Escape, S.R. = Synaptic Release, S.E. = Synaptic Escape.

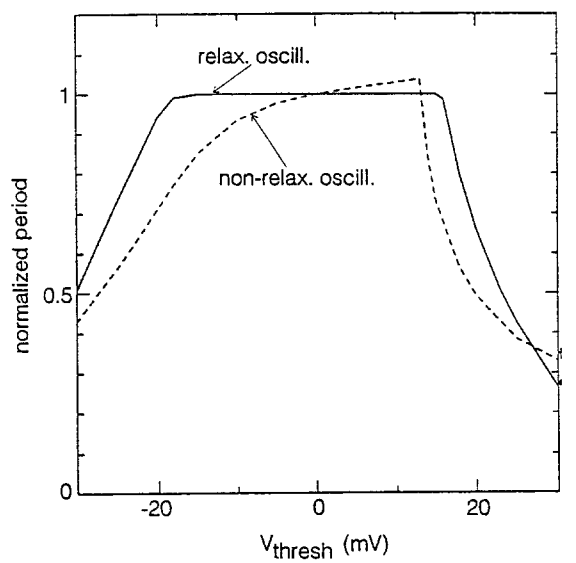

Fig. 9. Normalized period versus synaptic threshold voltage (V_{thresh}) for relaxation and non-relaxation like oscillations and steep synaptic activation slopes. The period is normalized to 1 at 0 mV synaptic threshold voltage. The solid line represents the relaxation like oscillations and the model parameters are the same as in Figure 4. The dashed line represents the non-relaxation like oscillations and ϕ_N = 0.002 msec^{-1}, 3 orders of magnitude larger.

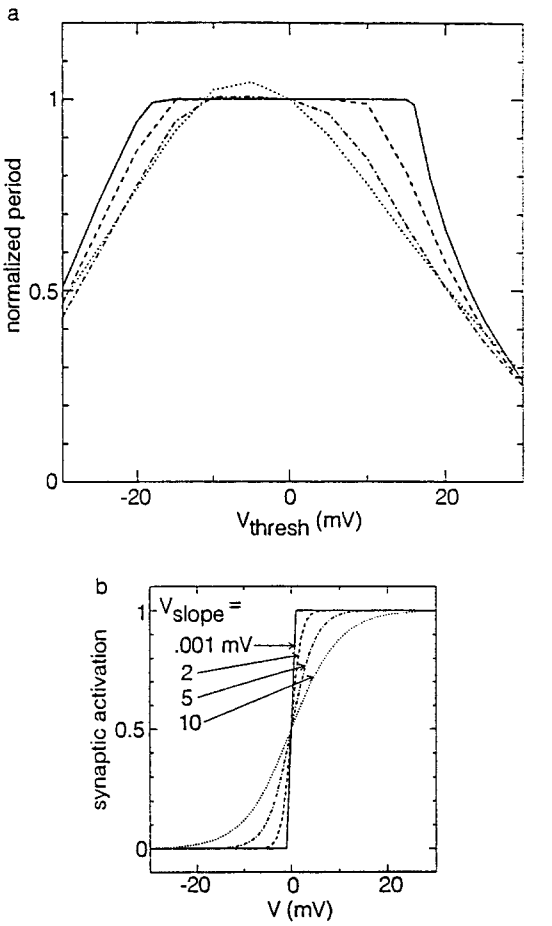

Fig. 10. (a) Normalized period versus synaptic threshold voltage (V_{thresh}) for the 4 different synaptic activation slopes shown in (b). The period is normalized to 1 at 0 mV synaptic threshold voltage. The model parameters are the same as in Figure 4 but with V_{slope} values of 0.001, 2, 5, 10 mV. (b) Synaptic activation versus voltage for 4 V_{slope} values of 0.001, 2, 5, 10 mV and a synaptic threshold of 0 mV.

case the synaptic activation changes from 0 to 1 very sharply. In comparison, the least steep slope is described by the dotted line (V_{slope} = 10 mV), and the synaptic activation takes about 60 mV to change from 0 to 1 (i.e., about 30 mV on either side of a 0 mV synaptic threshold).

Figure 10a shows plots of normalized period versus synaptic threshold for the four synaptic activations shown in Figure 10b. Again, these cases correspond to the nullclines exhibited in Figures 4a, 5a or 7a. As in previous figures, the period is normalized to 1 when the synaptic threshold is 0 mV. From Figure 10a, it is

clear that as the synapse becomes less steep, the distinction between intrinsic and synaptic mechanisms becomes less sharp. This is easy to understand since if the synapse is not very steep, then the particular cell will not be entirely free or inhibited above or below the synaptic threshold respectively. Instead, each cell will experience some partial inhibition depending on how far removed its partner is from the synaptic threshold. In other words, the $F = 0$ nullcline will be changing in time.

As the synapse becomes less steep, the range of synaptic threshold voltages for which there is no change in frequency decreases. The range of constant frequency is decreased by the range of voltages over which the synapse takes to activate from 0 to 1. As an example, consider the synaptic activation described by the dashed line in Figure 10b (V_{slope} = 2 mV). In this case, the synapse takes approximately 10 mV (or 5 mV on either side of a synaptic threshold of 0 mV) to activate from 0 to 1. When the corresponding normalized period versus synaptic threshold curve is considered in Figure 10a, we see that the range of synaptic threshold voltages for which there is no variation in period has decreased by about 10 mV, 5 mV on each side of the non-changing frequency region. This observation implies that if the voltage range that the synapse takes to activate from 0 to 1 is wider than the range of synaptic threshold voltages for which no frequency change is observed (when the synaptic activation is very steep), then there should not be a region of non-changing frequencies for this particular synaptic activation. This is illustrated for the example described by the dotted curves (V_{slope} = 10 mV) in Figure 10.

A Motivating Example

The determination of the mechanisms described above was motivated by a previous paper (Skinner et al., 1993) in which the behaviour of two cell reciprocally inhibitory networks were simulated. In that paper we considered how network behaviour and the frequency of network oscillations were influenced by injected current. We found that it was possible to start, stop and restart network oscillations as the amount of depolarizing current injected into each cell was increased. This behaviour is shown in Figure 11a (which is similar to Figure 13 in Skinner et al., 1993). In Figure 11b, we show phase plane portraits which correspond to the five levels of injected current values shown in Figure 11a. In each phase plane of Figure 11b, the sigmoidal and cubic-like curves are the nullclines and the dashed line represents the synaptic threshold voltage. As the injected current levels are changed, the phase plane portraits (i.e., nullclines and trajectories) also change. In these simulations, the synaptic threshold voltage is unchanged.

For the first two levels of injected current, the individual, uninhibited network elements are capable of autonomous oscillations. In addition, since the synaptic threshold is located between the upjump and downjump voltages of the coupled system, the mechanism for oscillation in these first two cases can be identified as intrinsic release.

For the first intrinsic release mechanism an interesting behaviour is observed: The trajectory of the inhibited cell is temporarily closer to the free voltage nullcline. This results in a jump from one hyperpolarized voltage to a more hyperpolarized region. This behaviour can be seen in Figure 11a for the first level of injected current shown. An analogue of this for the relaxation regime is discussed at the end of this section.

At the third level of injected current shown, the network does not oscillate. Instead bistable behaviour is exhibited with one cell in a hyperpolarized state and the other in a depolarized state. In this scenario, since neither the free nor inhibited cell systems are capable of exhibiting autonomous oscillations and the synaptic threshold voltage does not lie on the upper branch of the uninhibited nullcline or the lower branch of the inhibited nullcline, synaptic mechanisms cannot come into play.

With a further increase in injected current, network oscillations are again possible via the intrinsic escape mechanism. This is shown by the fourth case in Figure 11. The phase plane portrait is changed sufficiently so that now the inhibited cell system is capable of exhibiting au-

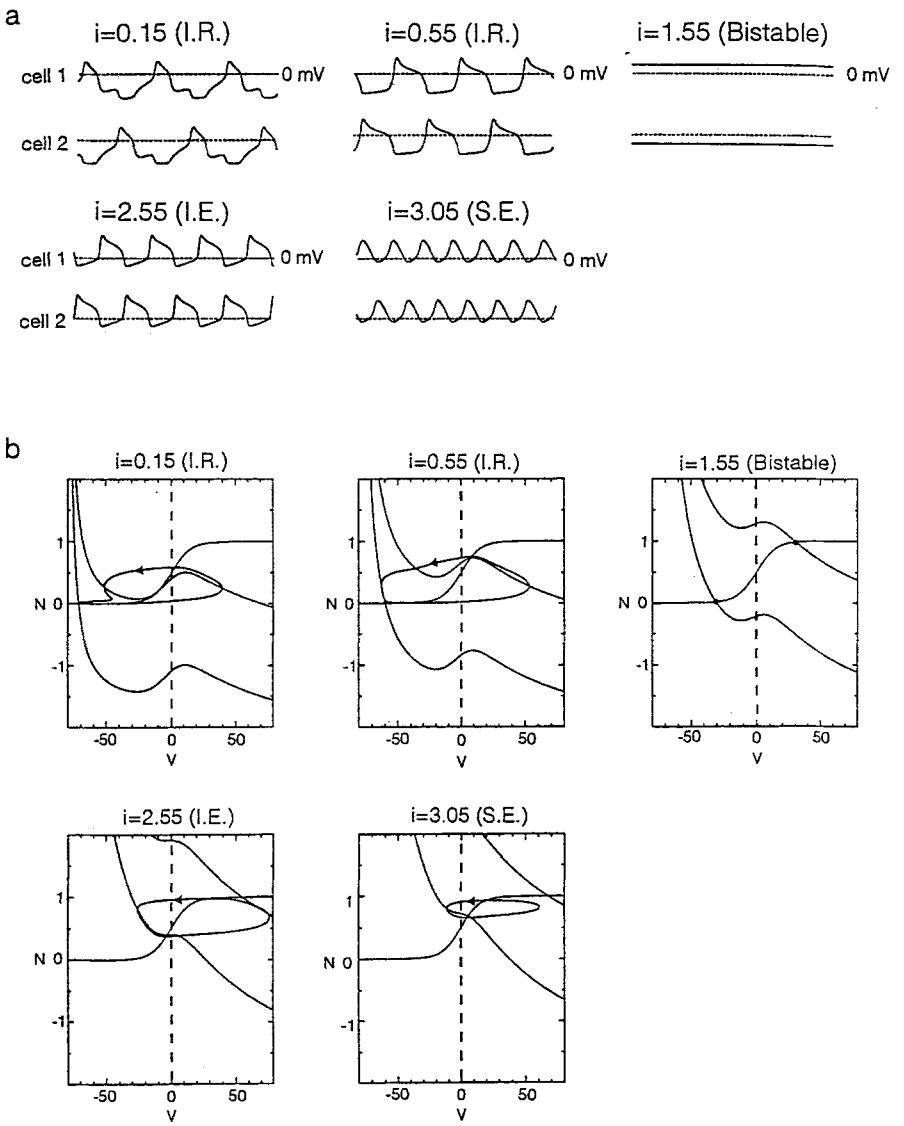

Fig. 11. (a) Voltage waveforms for a 2 cell reciprocally inhibitory network at 5 values of injected current. The parameters used are: $g_{syn} = 30\ \mu S/cm^2$, $\phi_N = 0.002\ msec^{-1}$, $V_{thresh} = 0$, $V_{slope} = 15$ mV. I_{ext} values are shown in the figure as i. See Appendix A for other parameter values. (b) Phase-plane portraits for the 5 levels of injected current shown in (a). There are two V-nullclines (cubic-like) representing the free and inhibited systems and one N-nullcline (sigmoidal-like). The dashed line represents the synaptic threshold voltage, and the trajectory is shown. I.R. = Intrinsic Release, I.E. = Intrinsic Escape, S.E. = Synaptic Escape.

tonomous oscillations, and the unchanged synaptic threshold is located between the upjump and downjump voltages of the coupled system.

As the injected current level is increased further, we get to the fifth case. Rhythmic behaviour in the network is still present but the underlying mechanism is now different. The unchanged synaptic threshold is now close enough to the lower branch of the inhibited voltage nullcline to allow oscillations via the synaptic escape mechanism. In these simulations, the synaptic activation is not very steep, and the oscillations are not of relaxation type. Therefore, the transition between the different mechanisms are not sharp.

For the third, fourth and fifth cases, the indi-

vidual, uninhibited cells are not capable of exhibiting autonomous oscillations. Several possible behaviours are shown for these cases: bistability and oscillations via an intrinsic escape or a synaptic escape mechanism. Since the individual, uninhibited cells are not capable of oscillatory behaviour, the oscillations are an emergent property of the network.

This example illustrates that the properties of the individual network elements and the synaptic couplings, as well as the network configuration, can result in the use of different mechanisms for oscillation.

As described above, the simulations given in Figure 11 have some different features from the periodic solutions constructed for our four mechanisms. One is that the simulations were not done in the relaxation range, and the other is that the simulations exhibit solutions with jumps from a hyperpolarized voltage to a more hyperpolarized one. The latter feature can be reproduced for solutions in the relaxation regime, provided that we consider solutions with duty cycles different from 1/2. As shown in Figure 12a, for the intrinsic release mechanisms in the relaxation regime, we can obtain voltage versus time plots in which there is a jump from one hyperpolarized voltage to a more hyperpolarized voltage for one of the cells and a jump from one hyperpolarized voltage to a less hyperpolarized voltage for the other. The singular solution associated with this is discussed in Appendix B.

Similarly, for the intrinsic escape mechanism in the relaxation regime, we can obtain voltage versus time plots in which there is a jump from one depolarized voltage to a more depolarized voltage for one of the cells and a jump from one depolarized voltage to a less depolarized voltage for the other cell. This is shown in Figure 12b. In both of these cases, the duty cycle is different from 1/2. For the simulations shown in Figure 12, in addition to the oscillations being in the relaxation regime, the synaptic activation was steep.

In Figure 12b, the duty cycle is greater than 1/2. This means that there is a region of overlap of firing for the two cells, despite the mutual inhibition. For leech heart interneurons, there are experimental observations which show that such

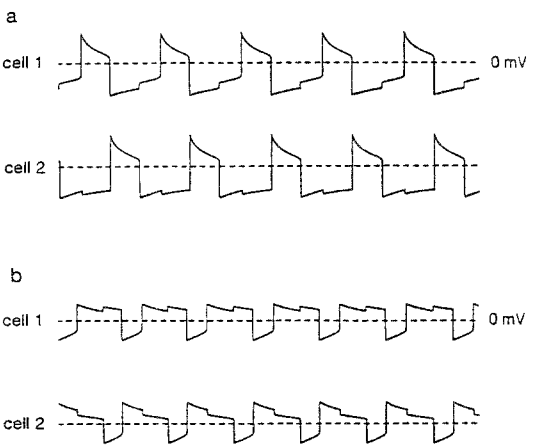

Fig. 12. Duty cycle $\neq$ 1/2. (a) Intrinsic release mechanism. Voltage versus time for the two cells using g_{syn} = 2.5 μS/cm^2, ϕ_N = 0.000002 msec^{-1}, V_{thresh} = 0, V_{slope} = 0.001 mV, and I_{ext} = 0.15 μA/cm^2. See Appendix A for the other parameters. (b) Intrinsic escape mechanism. Voltage versus time for the two cells using the same parameters as in (a) except I_{ext} = 0.78 μA/cm^2.

an overlap exists for two reciprocally inhibitory neurons (e.g. Calabrese and DeSchutter, 1992). Such an overlap could not be reproduced in a one-compartment model of a heart interneuron containing all identified ionic currents (Calabrese and DeSchutter, 1992; DeSchutter et al., 1993). However, as pointed out by the authors, this could be caused by several factors such as the non-inclusion of spike-mediated synaptic transmission.

Discussion

Neuromodulators are able to influence the output from neural networks by altering the intrinsic properties of the neurons or by changing the synaptic properties in the circuit (Harris-Warrick and Marder, 1991). In this paper we have given a clear indication of how the frequency of a two cell reciprocally inhibitory network is controlled by both intrinsic and synaptic properties.

Reciprocal inhibition between neurons is a common occurrence in many networks. Some examples include the pyloric and gastric networks of crustacea (Selverston and Moulins, 1987), the leech heartbeat network (Arbas and Calabrese, 1987), the swimming networks in ma-

rine molluscs and vertebrate embryos (Arshavsky et al., 1993; Satterlie, 1985), and the escape swim response in sea slugs (Getting, 1989b). In these networks, the individual cells may or may not exhibit oscillatory behaviour. For example, endogenous pacemaker activity has been recorded in isolated marine mollusc neurons (Arshavsky et al., 1993), but no intrinsically bursting neurons have been found in the leech heartbeat network (Calabrese and DeSchutter, 1992). As described in this paper, individual neurons with the ability to oscillate in the absence of inhibition can use the release mechanisms and individual neurons with the ability to oscillate under sustained inhibition can use the escape mechanisms.

It is important to realize that the mechanism for the generation of oscillatory behaviour in two cell reciprocally inhibitory networks can easily change. As shown in the previous section, changing the level of current injected into the two cells changes the mechanism by which oscillations are generated. In our simulations, any model parameter which alters the phase plane portrait could lead to a change in the operating mechanism, since the location of the nullclines relative to the synaptic threshold could change. For example, increasing the synaptic strength leads to a lowering of the voltage nullcline for the inhibited system. This could alter the mechanism by which network oscillations are generated or prevent oscillations from being produced.

The clear distinction between intrinsic and synaptic mechanisms disappears if the synapses are not steep. In the plot of period versus synaptic threshold, there is a transition between the portion with positive slope (frequency decreasing) and the portion with negative slope (frequency increasing). See dotted line in Figure 10a. In regions close to this transition, both intrinsic and synaptic mechanisms are in operation, and modulating either intrinsic or synaptic properties can easily cause a switch between release and escape mechanisms. However, in regions far from this transition, synaptic mechanisms dominate and a switch between release and escape mechanisms is unlikely.

In preliminary experiments these mechanisms were investigated with leech heartbeat interneurons. These neurons are naturally connected by chemical inhibitory synapses and form a half-center oscillator (Calabrese and DeSchutter, 1992). After pharmacologically blocking the natural synapses, the dynamic clamp (Sharp et al., 1993) was used to introduce artificial inhibitory chemical synapses between the leech neurons, and the synaptic threshold was varied. These experiments showed that the network period either increased or decreased as the synaptic threshold was artificially decreased (Skinner et al., 1994). This suggests that either synaptic release or synaptic escape modes dominate in determining network frequency under these experimental conditions, although under other conditions, intrinsic properties may play a stronger role.

In reciprocally inhibitory networks whose individual neurons do not exhibit autonomous oscillations, the property of postinhibitory rebound (PIR) in individual cells has been found to be adequate to generate oscillatory behaviour. This property has been exploited in several model studies (Calabrese and DeSchutter, 1992; Perkel and Mulloney, 1974; Wang and Rinzel, 1992). Wang and Rinzel (1992) used a quantitative model of the T-type calcium current in thalamic neurons which is strongly inactivated at rest. Hyperpolarization of sufficient amplitude and duration can then deinactivate this current. Calabrese and DeSchutter (1992) included a sag or hyperpolarization-activated inward current in their model and Perkel and Mulloney (1974) specifically included a PIR variable which is augmented with the arrival of inhibitory postsynaptic potentials. As shown here and in other simulations (LoFaro et al., 1994; Rowat and Selverston, 1993), the inclusion of a specific PIR-like current is not required to obtain oscillations in networks of reciprocally inhibitory cells in which the individual cells do not exhibit oscillatory behaviour. The mechanisms in this paper are described in terms of the intrinsic and synaptic properties of the neurons, and do not rely on the inclusion of specific currents. However, PIR (and other cellular properties) could alter the ability of an individual cell to exhibit autonomous oscillations with or without constant inhibition and so alter the operating mechanism in the system.

The mechanisms that we have described can be considered as an expansion of the work initiated by Wang and Rinzel (1992). These authors limited themselves to nonoscillatory cells that do not exhibit all the mechanisms described in this paper. In their work, they identified two mechanisms for oscillations in two cell reciprocally inhibitory networks. In the first mechanism, release, the inhibition is turned off allowing the inhibited cell to fire. In the second mechanism, escape, the inhibited cell "escapes" from the maintained inhibition. In addition they observed the following: For the release case, the network frequency was found to be very dependent on the synaptic threshold whereas for the escape case, the network frequency was relatively insensitive to the synaptic threshold. This is true only if *synaptic* release and *intrinsic* escape are the only mechanisms considered.

Despite the generality of our mechanisms, there are several shortcomings which should be highlighted. In our two cell reciprocally inhibitory model network, we assumed that the two cells had identical properties and that the coupling was symmetric. This is clearly not the case for many biological neurons. However, we believe that our analysis can be shown to be valid provided that the cells are not too different and the coupling is close to symmetric, as has been shown by Kopell and Somers (in preparation) for excitatory synaptic coupling. Additionally, we did not relax the assumption of a fast time constant for the synaptic coupling. This was considered by Wang and Rinzel (1992) who were able to obtain synchronous oscillations for the two cells if the synapses decay slowly.

We feel that the mechanisms described here provide a clear picture of some basic principles underlying pattern generation in reciprocally inhibitory model networks. As we remove assumptions such as symmetric coupling and consider larger networks, we hope to uncover further principles governing network behaviour.

Acknowledgments

We would like to thank the reviewers for their helpful and thorough comments on this work. This work was supported by NSF grant BNS9009251, NIMH grant MH-46742, NSF grant DMS- 9200131 and NIMH grant MH-47150.

Appendices

A. Model Equations

For the simulations shown in this paper, we use the Morris-Lecar model (Morris and Lecar, 1981). The basic model consists of two voltage dependent conductances and a leak current. In addition, we include an inhibitory synaptic current. The equations for cell 1 are shown below:

$$C\frac{dV^1}{dt} = I_{ext} - (g_L(V^1 - V_L) + g_{Ca}M^1_\infty(V^1 - V_{Ca}) + g_K N^1(V^1 - V_K) + g_{\text{syn}}S^1_\infty(V^1 - V_{\text{syn}})) \quad (2)$$

$$\frac{dN^1}{dt} = \lambda^1_N(N^1_\infty - N^1) \quad (3)$$

and

$$M^1_\infty(V^1) = \frac{1}{2}\left(1 + \tanh\left(\frac{V^1 - V_1}{V_2}\right)\right) \quad (4)$$

$$N^1_\infty(V^1) = \frac{1}{2}\left(1 + \tanh\left(\frac{V^1 - V_3}{V_4}\right)\right) \quad (5)$$

$$\lambda^1_N(V^1) = \phi_N \cosh\left(\frac{V^1 - V_3}{2V_4}\right) \quad (6)$$

$$S^1_\infty(V^2) = \frac{1}{2}\left(1 + \tanh\left(\frac{V^2 - V_{\text{thresh}}}{V_{\text{slope}}}\right)\right) \quad (7)$$

where
C = capacitance,
V = membrane voltage,
I_{ext} = external or imposed current,
g_L, g_{Ca}, g_K = leak, Ca^{2+} and K^+ maximal conductances respectively,
V_L, V_{Ca}, V_K = reversal potentials for the leak, Ca^{2+} and K^+ conductances respectively,
M_∞, N_∞ = fraction of open Ca^{2+} and K^+ channels at steady-state respectively,
N = fraction of open K^+ channels with a rate constant of opening given by λ_N,
ϕ_N = minimum rate constant for K^+ channel

opening,
V_1 = voltage at which half of the Ca^{2+} channels are open at steady-state,
V_2 = voltage whose reciprocal is the slope of voltage dependence of the fraction of open Ca^{2+} channels at steady-state,
V_3 = voltage at which half of the K^+ channels are open at steady-state,
V_4 = voltage whose reciprocal is the slope of voltage dependence of the fraction of open K^+ channels at steady-state,
g_{syn} = maximal synaptic conductance,
V_{syn} = reversal potential of the synaptic current,
S_∞ = fraction of open synaptic channels at steady-state,
V_{thresh} = voltage at which half of the synaptic channels are open at steady-state,
V_{slope} = voltage whose reciprocal is the slope of voltage dependence of the open synaptic channels at steady-state.
The superscripts refer to cell 1 or 2 in the network. For the reciprocally inhibitory coupling, the fraction of open synaptic channels of cell 1 is dependent on the voltage of cell 2, and vice-versa. Note that the activation of g_{Ca} is assumed to be instantaneous, or significantly faster than the activation of g_K. The synaptic activation is also assumed to be fast. The equations for cell 2 are similar.

With small values of V_{slope} the slope of the synaptic activation is very steep. This implies that above the threshold value, V_{thresh}, the inhibition is off, and below the threshold value the inhibition is on. Also, for small values of ϕ_N the oscillatory behaviour exists in the relaxation mode, i.e., the voltage trajectories stay close to the nullclines on the phase plane portrait. Numerical integrations are performed using LSODE, a double precision subroutine capable of handling stiff systems of first order ordinary differential equations, which is based on the Gear method (Gear, 1971).

In the table below, the parameter values used in the simulations are shown:

Parameter	Value	Units
g_K	20	$\mu S/cm^2$
g_{Ca}	15	$\mu S/cm^2$
g_L	5	$\mu S/cm^2$
V_{Ca}	100	mV
V_K	−80	mV
V_L	−50	mV
V_{syn}	−80	mV
C	1	$\mu F/cm^2$
V_1	0	mV
V_2	15	mV
V_3	0	mV
V_4	15	mV
g_{syn}, ϕ_N, I_{ext}		as in Figure
V_{slope}, V_{thresh}		as in Figure

B. Some Mathematical Details Concerning Existence and Stability of the Singular Solutions

In the limit $\epsilon \to 0$, approximate solutions to the coupled system can be calculated explicitly. These trajectories, known as singular solutions, are the union of solutions to a pair of reduced equations. The "slow system" associated with the coupled oscillators has the form:

$$\dot{N}_1 = g(V_1, N_1); \quad \dot{N}_2 = g(V_2, N_2). \qquad (8)$$

In (8), the values of V_i are functions of the N_i which satisfy the implicit constraints $f(V,N) = 0$ or $F(V,N) = 0$. Each of the latter two equations has a pair of relevant solutions corresponding to the left hand branch (LHB) and right hand branch (RHB). Thus, (8) describes the flow of each of the cells along some branch of the cubic $f = 0$ or $F = 0$. The construction of the singular solution consists of choices of solutions to (8) which, along with instantaneous jumps between them, fit together in a consistent manner.

The trajectories drawn in Figures 3a, 4a, 5a and 7a are singular solutions. We have previously described the conditions on the system for a trajectory with duty cycle 1/2 to exist in each of the four cases. We now give more details about the existence and stability of those trajectories.

We may ask whether there can be more than one such trajectory in each case, i.e., whether there is more than one point p which satisfies the time constraints discussed previously. Though we cannot prove that there is only one, we can show that the solution in each case is *locally* unique; i.e., there are no points p' near p for which the time constraints are satisfied. Both

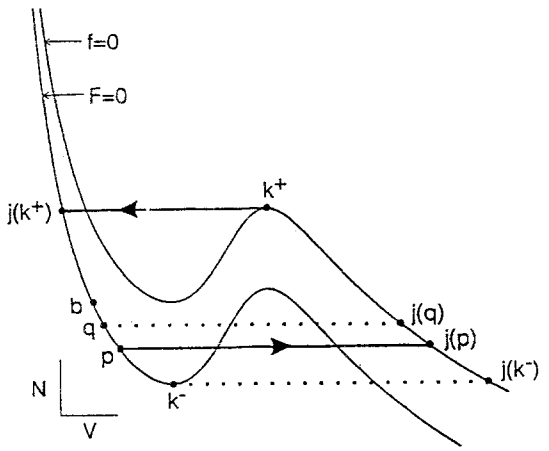

Fig. A1. Compression in the Intrinsic Release Mechanism. For any subinterval I between k^- and b, the time to traverse I is larger than the time to traverse the corresponding interval on the RHB of $f = 0$ between $j(k^-)$ and $j(b)$.

the local uniqueness and stability follow from a property of the Morris-Lecar equations that is shared by other voltage-gated conductance equations. This is the property of "compression" across jumps (Somers and Kopell, 1993), which we will illustrate in the context of the different mechanisms.

For definiteness, we discuss intrinsic release; intrinsic escape is parallel. The singular solution is as in Figure A1, which is very similar to Figure 3a. The "compression" condition we shall use was proved for the Morris-Lecar equations in some parameter ranges (Somers and Kopell, 1993) and concerns the range of points p on the LHB of $F = 0$ for which there could be a trajectory with duty cycle 1/2. For the intrinsic release mechanism, this is the interval between b and k^- (or b and the intersection of $F = 0$ with $g = 0$ if this intersection is on the LHB). We require that, for each subinterval I of this range, the image $j(I)$ on the RHB of $f = 0$ takes less time to traverse than I. (See Figure A1).

To see that this compression implies local uniqueness, consider a point q near p, say above p for definiteness. By compression, the time from q to p is larger than the time from $j(p)$ to $j(q)$. It follows from the definition of p that the time from $j(q)$ to k^+ must be greater than the time from $j(k^+)$ to q. Now consider a trajectory with oscillator 1 starting at k^+ and oscillator 2 starting at q. Oscillator 1 immediately jumps to $j(k^+)$, and oscillator 2 jumps to $j(q)$. It follows from the above arguments about times that when oscillator 2 reaches k^+, oscillator 1 will reach a position between q and p. This defines a map on the interval $[q,p]$ for which fixed points correspond to singular periodic orbits. Our argument shows that the only fixed point in this interval is the point p.

The existence of a singular solution does not automatically guarantee the existence of a nearby solution to the full $\epsilon \neq 0$ system. In our equations, however, the actual solution *is* guaranteed, provided the compression hypothesis holds. This is proved using the work of Mishchenkov and Rosov (1980), as refined by Bonet (1987). The compression also implies that the $\epsilon \neq 0$ solution is asymptotically stable and locally unique.

A similar argument works for intrinsic escape. In this case, the compression condition is placed on the interval on the RHB of $f = 0$ between the local maximum of the $f = 0$ curve (or the intersection with $g = 0$) and the point on the RHB of $f = 0$ at the same height as the local maximum of $F = 0$. For each subinterval of this, the jump to the LHB of $F = 0$ should compress the time it takes to traverse the interval. As before, this compression implies local uniqueness and stability. A similar analysis applies to the synaptic mechanisms.

The above analysis does not address the question of whether there *is* a point p with the right properties for any of the mechanisms. Consider, for example, the intrinsic release mechanism, as in Figure 3a. For the Morris-Lecar equations, the time from $j(k^+)$ to k^- on $F = 0$ is greater than the time from $j(k^-)$ to k^+ on $f = 0$. Furthermore, moving the point p upward from $p = k^-$ toward $p = b$ makes the times of traversal more equal. (This is a consequence of the compression described above.) This suggests that for some parameter ranges there should be a point p satisfying the time constraints imposed by requiring that the duty cycle be 1/2. The numerical simulations show that there are indeed some parameter ranges in which this is true. However, under the constraint that the

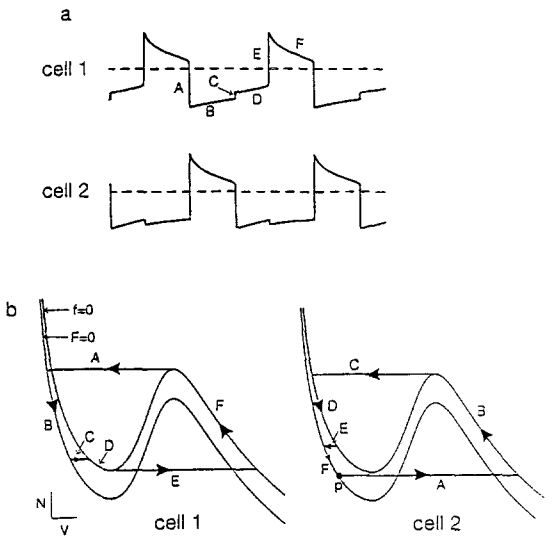

Fig. A2. (a) A portion of Figure 12, expanded and labelled. Figure 12 comes from a simulation in the relaxation regime, so the behaviour corresponds to some singular solution. (b) The phase plane diagram for oscillators 1 and 2, showing the singular solution corresponding to Figure 12. The labels on the diagrams correspond to the labels in Figure A2a. For example, in part A, oscillator 1 jumps downward and oscillator 2 jumps to the excited branch. In part B, oscillator 2 traverses the excited branch, arriving at the maximum point before oscillator 1 reaches point b on $F = 0$. When oscillator 2 jumps downward (part C), oscillator 1 jumps from the $F = 0$ nullcline to the $f = 0$ nullcline, but stays on the LHB of the latter; oscillator 2 goes to the nullcline $f = 0$ because that oscillator is also not receiving inhibition. In a similar way, the rest of the trajectory can be traced out and seen to be compatible with the rule that the choice of nullcline of each oscillator depends on whether or not it is receiving inhibition from the other. The point p is chosen so that the total time around the cycle is the same for the two oscillators.

duty cycle be 1/2, the point p may be varied only within the interval between k^- and b, and there may be no point p in that interval satisfying the time constraints. In that case the coupled system has solutions that do not correspond to duty cycle 1/2.

To understand what may happen, we consider the case of intrinsic release and assume that there is no point p between k^- and b for which the time from $j(p)$ to k^+ is equal to the time from $j(k^+)$ to p. It is still possible to obtain a singular solution in which no more than one of the oscillators lies on a RHB at any given time. Figure A2 illustrates such a situation. In Figure A2a, the voltage versus time plot of Figure 12a is shown, with different parts of the cycle labelled A through F. In Figure A2b the phase plane diagram is given for both oscillators, with each part of the cycle labelled to correspond to voltage/time plot of Figure A2a. As shown in Figures A2a,b, in this regime the two oscillators do not follow the same path in phase space, and they do not have the same voltage versus time behaviour.

A similar analysis can be done for the intrinsic escape case, to produce phase plane diagrams corresponding to Figure 12b. In this case, there *is* an interval of overlap in firing, but there is no more than one oscillator on a LHB at any given time.

References

Arshavsky YI, Orlovsky GN, Panchin YV, Roberts A, Soffe SR (1993) Neuronal control of swimming locomotion: analysis of the pteropod mollusc *Clione* and embryos of the amphibian *Xenopus*. TINS 16:227–233.

Arbas EA, Calabrese RL (1987) Slow oscillations of membrane potential in interneurons that control heartbeat in the medicinal leech. J. Neurosci. 7:3953–3960.

Bonet C (1987) Singular perturbation of relaxed periodic orbits. J. Diff. Eqns. 66:301–339.

Brown TG (1911) The intrinsic factors in the act of progression in the mammal. Proc. Roy. Soc. Lond. B 84:308–319.

Calabrese RL, DeSchutter E (1992) Motor-pattern-generating networks in invertebrates: modeling our way toward understanding. TINS 15:439–445.

Cohen AH, Rossignol S, Grillner S, eds (1988) Neural Control of Rhythmic Movements in Vertebrates. John Wiley and Sons Inc. New York.

Delcomyn F (1980) Neural basis of rhythmic behaviour in animals. Science 210:492–498.

DeSchutter E, Angstadt JD, Calabrese RL (1993) A model of graded synaptic transmission for use in dynamic network simulations. J. Neurophysiol. 69:1225–1235.

Gear CW (1971) Numerical Initial Value Problems in Ordinary Differential Equations. Prentice-Hall Inc, Englewood Cliffs, New Jersey.

Getting PA (1989a) Emerging principles governing the operation of neural networks. Ann. Rev. Neurosci. 12:185–204.

Getting PA (1989b) A network oscillator underlying swimming in *Tritonia*. In: Jacklet JW, ed. Neuronal and Cellular Oscillators. Marcel Dekker Inc., New York.

Harris-Warrick RM, Marder E (1991) Modulation of neural networks for behavior. Ann. Rev. Neurosci. 14:39–57.

Jacklet JW, ed (1989) Neuronal and Cellular Oscillators. Marcel Dekker Inc., New York.

Kopell N, Somers, D (1993) Anti-phase solutions in relaxation oscillators coupled through excitatory interactions. (submitted).

Llinás RR (1988) The intrinsic electrophysiological properties of mammalian neurons: Insights into central nervous system function. Science 242:1654–1664.

LoFaro T, Kopell N, Marder E, Hooper SL (1994) Subharmonic coordination in networks of neurons with slow conductances. Neural Comp. 6:69–84.

Marder E (1993) Modulating membrane properties: role in information processing. In: Poggio TA, Glaser DA, eds., Exploring Brain Functions: Models in Neuroscience. John Wiley and Sons Ltd. pp. 27–42.

Mishchenkov EF, Rosov N (1980) Differential Equations with Small Parameters and Relaxation Oscillations. Plenum Press, New York.

Morris C, Lecar H (1981) Voltage oscillations in the barnacle giant muscle fiber. Biophys. J. 35:193–213.

Perkel DH, Mulloney B (1974) Motor pattern production in reciprocally inhibitory neurons exhibiting postinhibitory rebound. Science 185:181–183.

Rowat PF, Selverston AI (1993) Modelling the gastric mill central pattern generator of the lobster with a relaxation-oscillator network. J. Neurophysiol. 70:1030–1053.

Satterlie RA (1985) Reciprocal inhibition and postinhibitory rebound produce reverbation in a locomotor pattern generator. Science 229:402–404.

Selverston AI, Moulins M (1985) Oscillatory neural networks. Ann. Rev. Physiol. 47:29–48.

Selverston AI, Moulins M eds (1987) The Crustacean Stomatogastric System. Berlin: Springer-Verlag.

Sharp AA, O'Neil MB, Abbott LF, Marder E (1993) Dynamic clamp: Computer-generated conductances in real neurons. J. Neurophysiol. 69:992–995.

Skinner FK, Gramoll S, Calabrese RL, Kopell N, Marder E (1994) Frequency control in biological half-center oscillators. In: Eeckman F, Bower JM, eds., Computation and Neural Systems. Kluwer Academic Publishers, Boston (In press).

Skinner FK, Turrigiano GG, Marder E (1993) Frequency and burst duration in oscillating neurons and two cell networks. Biol. Cyber. 69:375–383.

Somers D, Kopell N (1993) Rapid synchronization through fast threshold modulation. Biol. Cyber. 68:393–407.

Wang X-J, Rinzel J (1992) Alternating and synchronous rhythms in reciprocally inhibitory model neurons. Neural Comp. 4:84–97.